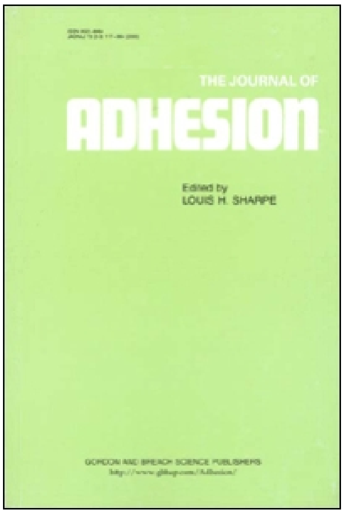

The Journal of Adhesion
Publication details, including instructions for authors and subscription information:
http://www.informaworld.com/smpp/title~content=t713453635

Photoelastic Stress Analysis of Bonded Lap Shear Joints Having Thermoplastic Adherends

Jessica A. Schroeder[a]
[a] Polymers Department, General Motors Research Laboratories, Warren, MI, U.S.A.

To cite this Article Schroeder, Jessica A.(1990) 'Photoelastic Stress Analysis of Bonded Lap Shear Joints Having Thermoplastic Adherends', The Journal of Adhesion, 32: 2, 89 — 103
To link to this Article: DOI: 10.1080/00218469008030183
URL: http://dx.doi.org/10.1080/00218469008030183

J. Adhesion, 1990, Vol. 32, pp. 89–103
Reprints available directly from the publisher
Photocopying permitted by license only

Printed in the United Kingdom

Photoelastic Stress Analysis of Bonded Lap Shear Joints Having Thermoplastic Adherends

JESSICA A. SCHROEDER

Polymers Department, General Motors Research Laboratories, Warren, MI 48090–9055, U.S.A.

(Received November 9, 1989; in final form March 26, 1990)

The effects of substrate stiffness and modulus on joint strength and stress distribution were investigated for a series of nylon substrates bonded with an epoxy adhesive. Substrate stiffness and modulus were controlled by the level of glass filler in the resin. Single lap shear samples having both identical ("self-bonded") and dissimilar ("cross-bonded") substrates were investigated. For the self-bonded samples, lap shear strength was found to increase with increasing substrate modulus and stiffness. The strengths of the cross-bonded samples were intermediate to the strengths of the corresponding self-bonded samples. Photoelastic techniques were used to observe stress patterns in the lap joints during testing. One type of stress pattern was observed for all self-bonded samples regardless of substrate stiffness. Two patterns, one for the stiff substrate and one for the more flexible substrate, were observed for cross-bonded samples. The photoelastic analysis agreed qualitatively with predictions of stress distributions based on linear elastic and linear elastic/perfectly plastic theoretical models.

KEY WORDS joint stress distribution; photoelastic stress analysis; thermoplastic bonding; mixed substrate bonding.

INTRODUCTION

Polymeric materials offer certain advantages, with respect to metals, for use in structural and semi-structural automotive applications. These advantages include weight savings, greater design and styling flexibility, part consolidation, better tooling efficiency, and improved energy management.[1] However, appropriate joining methods are required to use these engineering materials to their full potential. Adhesive bonding is just such a method, since it confers the ability to join dissimilar materials, and offers better strength-to-weight ratios and a more uniform stress distribution within a joint than mechanical fastening. It is necessary, however, to understand the properties of, and interactions between, a given substrate and adhesive in order to optimize joint performance. It is necessary, also, to understand the behavior of the joint as an integrated unit within an entire structure.

The effects of substrate stiffness and modulus on joint strength and stress distribution were investigated for a series of nylon substrates bonded with an expoy adhesive. By changing the level of glass filler in the nylon resin, substrate stiffness and modulus were varied systematically without significantly affecting substrate surface chemistry. Thus, the effects of the substrate bulk properties on the behavior of single lap joints could be evaluated independently of changes in substrate/adhesive interfacial interactions.

Photoelastic techniques were used to examine the stresses within the lap shear joints during testing. Photoelastic stress/strain analysis is a method whereby the surface strains in a test part can be observed and measured during static or dynamic loading. A thin layer of a birefringent material is bonded to the surface of the test part using a reflective adhesive. When the part is loaded, the strains on the surface of the part are transmitted to the birefringent coating through the adhesive. Then, when the part is viewed through a reflection polariscope, a series of black isoclinic and/or colored isochromatic fringes are observed. The principal strain directions in the part can be determined from the isoclinic pattern, while the overall stress/strain distribution is represented by the color pattern of the isochromatic fringes. As load is applied to the part, a colored fringe will appear in the region experiencing the highest stress. When the load is increased, the original fringe is replaced with a fringe (color) representing a higher stress/strain level, and the original fringe moves toward an area of lower stress. Fringe "orders" (N) increase with load, producing a contour map of stress and strain levels. The fringe pattern advances as follows: black (no load), yellow, red, purple, blue, yellow, red, purple, blue-green, yellow-green, red, green.[2] Note that, in this work, photoelastic analysis was used qualitatively. That is, only distribution patterns were obtained; actual values of stress and/or strain were not sought. Thorough discussions of the principles of photoelastic analysis may be found in references [3] and [4].

In addition to being a non-destructive technique, photoelastic analysis provides, with proper coating selection, the ability to test a wide range of elastic and plastic strain levels for many types of materials.[5] Even though the observed stress patterns are those of the surface of the part rather than the interior (in a bonded part, therefore, the stresses would not be those within the adhesive), photoelastic patterns do provide an indication of the stresses within a structure. Therefore, as an engineering and design tool, photoelastic stress analysis can be used to locate, and then eliminate, points of high stress concentration in a part, and to improve the "minimum weight to maximum function" relationship of a part, by identifying under-stressed or highly-stressed regions within the part.

Three nylon substrates were used in this investigation: unfilled nylon 6, 6 (UFN), 43% glass-filled nylon 6, 6 (GFN), and a 50/50 mix of the unfilled and 43% glass-filled resins (MN). Flexural stiffness, flexural modulus, and tensile modulus were obtained for each substrate. Lap shear joints having identical nylon adherends ("self-bonded") and joints having different (with respect to stiffness) adherends ("cross-bonded") were then prepared. Lap shear strengths and stress patterns were obtained. Joint strength was correlated with the three abovementioned substrate properties, and the photoelastic stress distribution patterns were compared with the stress patterns predicted by linear elastic[6] and linearly elastic/perfectly plastic[7] theoretical models.

EXPERIMENTAL

Materials

The adhesive used to join the lap shear coupons was a two-part epoxy, Fusor 320/322 (Lord Corporation). An aluminum-filled, two-part epoxy adhesive, PC-1/PCH-1 (Photolastic Division, Measurements Group, Inc.) was used to bond the photoelastic coating to the lap shear coupons.

The lap shear substrates were all based on nylon 6, 6. The unfilled nylon substrate, UFN, was molded from Zytel® 101L resin, while the 43% glass-filled substrate, GFN, was molded from Zytel® 70G43L resin. Both resins were supplied by DuPont and, having similar additives (lubricant only), should provide molded samples with similar surface chemistry. A 50/50 mix, by weight, of the 101L and 70G43L resins was used to prepare a substrate material (designated MN) with an intermediate level of glass filler. Resin pellets were dried and then molded into $10.2 \times 2.5 \times 0.31$ cm coupons using a New Britain 75 Injection Molding Machine. Coupons were stored in a desiccator until used.

The photoelastic coating used in this work was in the form of a fully-cured flat sheet (PS-2C, Photolastic Division of the Measurements Group, Inc.). The thickness of the clear coating was nominally 1 mm, the "K" factor, or strain-optic coefficient, was 0.13 (dimensionless), and the coating sensitivity, or fringe value f, was approximately 2200 μm/m per fringe.

Lap shear sample preparation

Nylon coupons were prepared for bonding by abrading with a Scotch Brite® pad (3 M), wiping with methylene chloride, and then allowing them to dry. The adhesive was hand mixed (10 g Fusor 320 with 12 g Fusor 322) and applied to the bond area with a spatula. Coupons were placed in a fixture designed to produce a bond overlap of 1.27 cm (0.5 in). The fixture was shimmed to produce a bond thickness of 0.3 mm (12 mil). A piece of 30 gauge copper wire was used as a spacer to help maintain bond thickness. Samples were then placed in a forced air oven for 20 min at 93°C to cure the adhesive. The samples were allowed to cool in the fixtures overnight, and then put through a simulated automotive paint bake cycle† on the following day. This paint bake cycle served as the adhesive post cure cycle. With reference to the terminology introduced above, UFN/UFN, MN/MN, and GFN/GFN self-bonded samples, and GFN/MN, UFN/MN, and

† Paint bake cycle: 30 min at 121°C; cool to room temperature; 30 min at 149°C; cool to room temperature; 60 min at 177°C; cool to room temperature; 15 min at 149°C; cool to room temperature; 35 min at 163°C; cool to room temperature; 30 min at 154°C; cool to room temperature.

UFN/GFN cross-bonded samples were prepared in this manner and stored in a desiccator until application of the photoelastic coating.

Photoelastic coating application

The PS-2C sheets were cut, using a jigsaw, into rectangles slightly larger than 2.5 × 5.0 cm. Before bonding PS-2C coating pieces to lap shear coupons, the coupons were abraded with a Scotch Brite® pad (3 M), wiped first with isopropyl alcohol, then with a 10% solution of ammonium hydroxide, after which they were allowed to dry. The coating pieces themselves were wiped with isopropyl alcohol and allowed to dry. A heat lamp was used to warm the PC-1 adhesive resin, 20 g of which was then hand mixed with 2 g PCH-1 hardener, and applied to the lap shear coupons with a spatula. The photoelastic coating was positioned on top of the adhesive, taking care to eliminate any air pockets between adhesive and coating (see Figure 1). After two hours at room temperature, excess adhesive was removed from the coating with acetone. The adhesive was then allowed to continue to cure, at room temperature, overnight. Finally, coating edges were ground to match the edges of the lap shear coupons using a sander with 280 grit paper (dry).

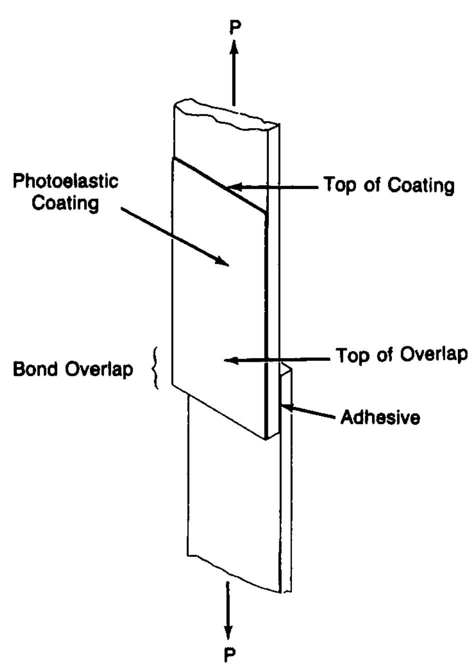

FIGURE 1 Diagram of lap shear coupon with photoelastic coating.

Substrate stiffness

The relative stiffness of both uncoated and coated (PS-2C) lap shear coupons was measured in 3-point bending for each of the three materials, UFN, MN, and GFN. The method for determining flexural stiffness was derived from ASTM D790. Using an Instron (Model TTC) Testing Machine, room temperature load *v.* deflection curves were obtained. Total specimen length, width, and thickness were those of the (coated or uncoated) lap shear coupons. The support span was 50 mm and the crosshead speed was 1.3 mm/min. Stiffness was determined by measuring the load sustained by the specimen, within the linear portion of the curve, at the greatest deflection common to all specimens. Note that stiffness is a function of geometry, so that values obtained here relate only to specimens of these dimensions.

Flexural modulus

The flexural modulus of each substrate was obtained, at room temperature, in accordance with ASTM D790 using an Instron (Model 1125) Universal Testing Machine. Nonbonded lap shear coupons were used as specimens.

Tensile modulus

Tensile dog-bone specimens of each nylon substrate were molded using a New Britain 75 Injection Molding Machine. The room temperature tensile modulus of each substrate was obtained in accordance with ASTM D638 using an Instron (Model 1125) Universal Testing Machine.

Lap shear/photoelastic testing

Coated lap shear samples were tested at room temperature, at a crosshead speed of 1.27 mm/min, using an Instron (Model TTC) Testing Machine. Peak loads were recorded, and the failure surfaces of the coupons visually examined. Failure modes are listed and defined in Table I.

TABLE I
Failure mode designations and definitions

Designation	Definition
ADH	Adhesional failure: failure at the substrate/adhesive interface
COH	Cohesional failure: failure within the bulk of the adhesive
SF	Substrate failure: failure of the substrate coupon
MIX	Mixed failure: adhesional and cohesional areas present on the same sample

A tripod-mounted, 030-Series Reflection Polariscope (Photolastic Division, Measurements Group, Inc.) was used to observe the isochromatic stress patterns in the coated, strained samples. A Panasonic video camera was mounted behind the polariscope analyzer such that the changing stress patterns during testing could be recorded. The diagrams of the stress patterns shown below (Figures 5 and 6) are reproductions of still photographs obtained from the videotape.

RESULTS

Lap shear strengths and substrate properties

Self-bonded samples. Lap shear strengths and failure modes of the coated, self-bonded nylon samples are listed in Table II. UFN samples exhibited substrate and cohesional failures (SF and COH), while the MN and GFN samples exhibited COH failures (see Table I for failure mode definitions). Lap shear strength increased in the order

$$\mathrm{UFN/UFN} < \mathrm{MN/MN} < \mathrm{GFN/GFN},$$

from 6600 ± 600 to 9500 ± 600 kPa. Based on the results of preliminary work performed in this laboratory, there was no significant difference between lap shear strengths of coated and uncoated samples. Thus, even though the addition of the photoelastic coating increased coupon stiffness (see below), the stiffness difference (coated minus uncoated) was not sufficient to affect lap shear results.

Table III lists the relative stiffness of the uncoated and coated nylon coupons. Clearly, substrate stiffness is greater with the addition of the coating. However, since the increase in stiffness is constant for all three nylon substrates ($\approx$ 0.12 kN/mm), the order of substrate stiffness, UFN < MN < GFN, is unchanged, as is the relationship between substrate stiffness and lap shear strength (compare Figure 2a and 2b). Therefore, in the latter sections of this paper, where the

TABLE II
Lap shear strengths and failure modes

Sample	Lap Shear Strength (kPa)	Failure Mode[a]
Self-Bonded Samples		
UFN/UFN	6600 ± 600	SF, COH
MN/MN	7500 ± 500	COH
GFN/GFN	9500 ± 600	COH
Cross-Bonded Samples		
GFN/MN	8100 ± 800	COH
UFN/MN	8600 ± 900	COH, SF
UFN/GFN	8000 ± 1000	COH, ADH, SF

[a] Failure modes are defined in Table I.

TABLE III
Relative substrate stiffness and substrate flexural and tensile moduli

Substrate	Relative stiffness, uncoated coupons (kN/mm)	Relative stiffness, coated coupons (kN/mm)	Flexural modulus (MPa)	Tensile modulus (MPa)
UFN	0.06 ± 0.01	0.170 ± 0.009	3000 ± 80	2900 ± 200
MN	0.12 ± 0.02	0.200 ± 0.009	5700 ± 300	6600 ± 600
GFN	0.22 ± 0.02	0.34 ± 0.01	11400 ± 300	12000 ± 2000

relationships between substrate stiffness, stress distribution patterns, and lap shear behavior are analyzed, the arguments are valid for both coated and uncoated samples.

Substrate flexural and tensile moduli are also listed in Table III, and the relationships between these substrate bulk properties and lap shear strength are illustrated in Figure 3(a and b). In sum, lap shear strength was found to increase as substrate stiffness (Figure 2) and substrate modulus increased. There does not appear to be a strong dependence of lap shear failure mode on any of the substrate bulk properties investigated.

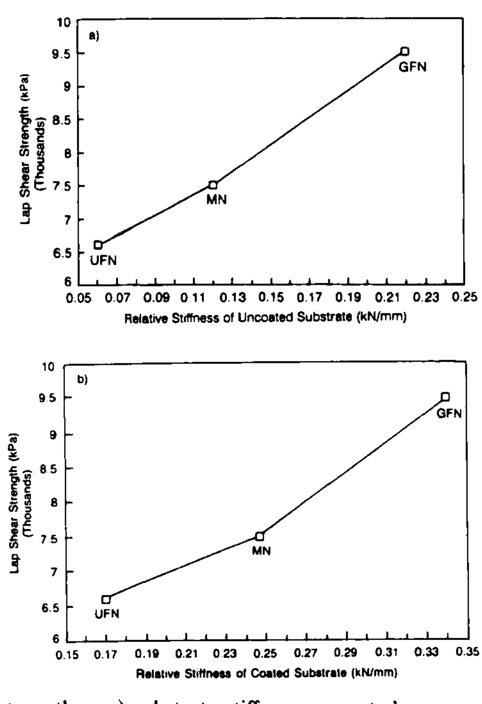

FIGURE 2 Lap shear strength *v*. a) substrate stiffness, uncoated coupons and b) substrate stiffness, coated coupons.

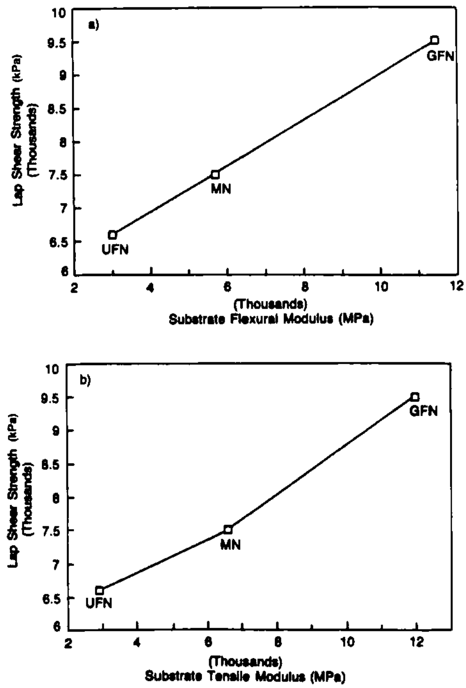

FIGURE 3 Lap shear strength *v.* a) substrate flexural modulus and b) substrate tensile modulus.

Cross-bonded samples. Table II lists the lap shear strengths and failure modes of the coated, cross-bonded nylon samples. Strengths varied from 6600 ± 900 to 8100 ± 800 kPa for these samples, with three types of failure (ADH, COH, SF) observed. The strengths of these cross-bonded samples exhibited a slight dependence on substrate stiffness. That is, cross-bonded samples with the highest stiffness substrate GFN/MN and UFN/GFN, had higher strengths than samples containing the lower stiffness substrates, UFN/MN.

Figure 4 compares the strengths of the cross-bonded samples with the strengths of the corresponding self-bonded samples. The figure suggests, even though standard deviation is significant for the cross-bonded samples (Table II), that the strengths of the cross-bonded samples are intermediate to the strengths of the corresponding self-bonded samples. This is in agreement with results from previous work in our laboratory involving nylon substrates bonded to themselves, and to other thermoplastics and metals.[8]

Isochromatic fringe patterns

Self-bonded samples. All of the self-bonded samples, UFN/UFN, MN/MN, and GFN/GFN, exhibited essentially the same isochromatic pattern during lap shear

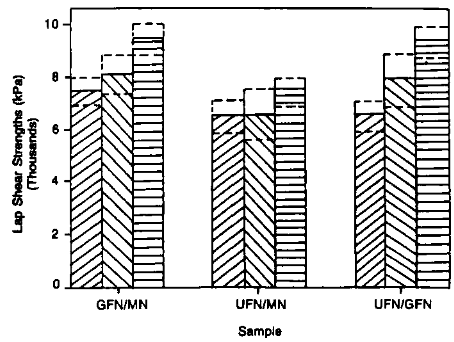

FIGURE 4 Lap shear strength of cross-bonded samples as compared with the strengths of corresponding self-bonded samples (the cross-bonded sample is represented by the center bar of each set, while the outer bars represent the strengths of the self-bonded samples). Dashed lines indicate standard deviation.

testing. The pattern developed, in stages, as follows (see Figure 5; each lettered diagram corresponds to the appropriate section of the description below):

The entire photoelastic coating appeared dark prior to loading (a). As load was applied, the area from the top of the coating to the top of the bond overlap brightened, became yellow and then purple (b). As loading continued, the coating over the overlap region also became yellow, and the coating at the edges (sides) of the coupons, directly above the top of the overlap, became first red, and then purple (c). Also at this stage of the test, a thin black line was noted in

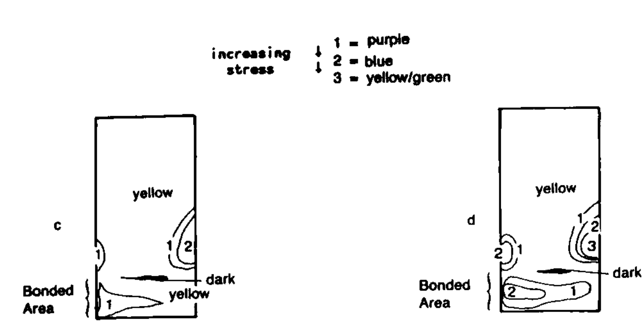

FIGURE 5 Scale diagram of photoelastic pattern 1 (see text for description of letters a-d).

the center of the coupon just below the top of the overlap area (c). As the spots at the coupon edges increased in size with increasing load, color began to develop in the coating over the center of the overlap region (d). The colored areas of the coating continued to expand, and the pattern repeated through two or three fringes (*i.e.*, the fringe orders, N, were $\simeq 2$–3) until failure occurred. This will be referred to as "pattern 1."

A certain amount of asymmetry in the stress patterns was noted. This is due to either uneven loading, a result of slightly off-center fixturing, or variations in the bond thickness of the sample.

Cross-bonded samples. Depending on substrate stiffness, one of two patterns was seen for the cross-bonded nylon samples. If the photoelastic coating was placed on the more flexible substrate of the pair, pattern 1 was observed. A second pattern was recorded when the stiffer substrate was coated (Figure 6):

Before load was applied, the photoelastic coating was dark (a). As load was applied, the area between the top of the coating and the top of the overlap, became yellow (b). As the test continued, the coating over the overlap region became yellow, and red and green lines developed, spanning the width of the coupon at the top of the overlap region (c). These lines moved down into the overlap region while red, and then green, spots developed at the edges of the coupon at the top of the overlap region (d). The lines running across the coupon continued to move down the coupon, and the spots continued to expand, until failure occurred. With the exception of UFN/GFN samples, which will be discussed in greater detail below, the color pattern cycled through approximately

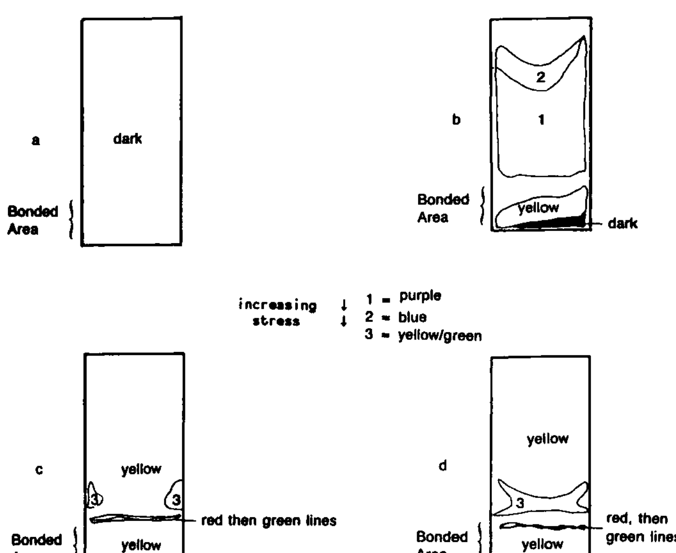

FIGURE 6 Scale diagram of photoelastic pattern 2 (see text for description of letters a-d).

three fringes for both substrates. Thus, fringe orders were, with the exception of the UFN/GFN samples, approximately 2–3. This will be referred to as "pattern 2."

DISCUSSION

Ideally, for a single lap joint whose adherends are loaded in tension, the adhesive in the joint is subjected only to shear stress. In reality, the stress state in a lap joint is considerably more complex. Models developed to describe the stress distribution within the lap joint have included not only the effects of longitudinal (*i.e.*, in the direction of the tensile load) shear stress, but also transverse shear and normal (peel) adhesive stresses, end effects, and yield and deformation for both adhesive and adherend. These models are reviewed in reference [9]. It is the stress distribution within the joint, specifically the location of stress concentrations in adhesive and/or adherend, which ultimately determines joint strength and failure mode.

Strength vs. stress distribution

Self-bonded samples. Linear elastic[6] and linear elastic/perfectly plastic[7] models may be used to interpret the lap shear data obtained in this work. Renton and Vinson,[6] using an elastic model, performed a parametric study of a single lap joint to determine the factors having significant effect on joint stress distribution. Their analysis was performed for both similar (self-bonded) and dissimilar (cross-bonded) adherends. According to the analysis, the shear stress distribution within the adhesive becomes more uniform, and peak normal stresses within the adhesive are reduced, as the primary elastic modulus of the adherend(s) is (are) increased. Also, the state of stress in an adhesive approaches pure shear as the in-plane and flexural stiffness of the adherends increase. Subsequent linear elastic analyses by Kline[10] and Kyogoku *et al.*[11] gave similar results.

Therefore, as substrate stiffness and modulus increased for the self-bonded nylon samples investigated in this work, peak stresses within the joints decreased and the stress distribution became more uniform (in shear), enabling the load-bearing capacity of the joints to increase. In addition, the models indicate that peak stresses for both adhesive and adherend occur at the ends or corners of the joint overlap.[9] Thus, while the models cannot differentiate between COH, ADH, and SF failure modes since high stress regions occur in both the substrate and adhesive, and at the interface, the models do suggest that bond failure initiates at the edges of the overlap.

Cross-bonded samples. Both linear elastic and linear elastic/perfectly plastic models predict that peak shear stress within the adhesive increases, and that the stress distribution within the adhesive becomes increasingly nonuniform, the greater the stiffness difference between substrates.[6,7] Also, adhesive shear stress is greatest at the end of the joint overlap on the side of the more flexible substrate. Maximum normal stress in the adhesive also occurs adjacent to the more flexible substrate. One would expect, then, that the strengths of the cross-bonded samples tested in this work would increase in order UFN/GFN < GFN/MN ≤ UFN/MN, as the difference in substrate stiffness and modulus values decreases. Although there is considerable scatter in the data (Table II), this does not appear to be the case; the GFN/MN and UFN/GFN had the same lap shear strengths, and the UFN/MN samples had the lowest strengths of the cross-bonded samples. Apparently, the decrease in peak shear and normal stresses which occurs when overall substrate stiffness is increased, is more important for the UFN/GFN samples than the increase in adhesive stresses due to substrate dissimilarity. The competing effects of substrate stiffness *vs.* substrate dissimilarity will be discussed, for the UFN/GFN samples, in more detail below.

Photoelastic stress analysis

Whereas theoretical models may predict general trends, photoelastic techniques may be used to examine, more directly, the stress (strain) distribution patterns of bonded joints during loading. Experimentally observed patterns can then be compared to model predictions. It must be noted, however, that the photoelastic patterns are those of the outer surface of the adherends. Thus, *adhesive* stress distribution, as predicted by the models discussed above, cannot be compared directly with photoelastic data.

Self-bonded samples. The following discussion applies to all self-bonded lap shear samples since they all displayed photoelastic pattern 1.

With initial load application, the lap shear coupons themselves were subjected to a tensile strain. Thus, as the adherend's stress pattern developed, color first appeared (in the coating) in the area between the Instron grips and the top of the overlap (Figure 5b). In the bonded region, the coupon is "reinforced," which defers the growth of strain into this area. As load was increased, however, tensile strain progressed into the bonded region of the coupon as evidenced by the appearance of the color (yellow) in this region. Since, as can be seen from Figure 1, applied tensile forces were not co-linear, the coupons next began to flex and bend. As the coupon flexed, higher fringe orders colors (red, purple, green) became visible at the top edges of the bond overlap (Figure 5c), indicating that these locations had the highest stresses (strains) in the joint. As noted above, this is the behavior predicted by the linear elastic/perfectly plastic model[7] of the stress in a single lap joint. Additionally, when viewing the video recording of the test in slow motion, it was possible to determine, in some cases, where failure began. The fringes reversed (*i.e.*, N decreased), and began to disappear, starting from the bottom edges of the lapped region of the samples. Again, assuming that failure will begin at the point(s) of highest stress, this failure initiation location was predicted by the model.

Two additional features of pattern 1 require an explanation. The first of these features is the black line which appeared in the center of the coupon just below the top of the overlap (Figure 5c). This suggests that there is a line of zero stress (strain) across the width of the coupon. This "node" may be caused by a change in the direction of the curvature of the coupon as it flexes with increasing load. The second feature requiring interpretation is the high stress (strain) region that develops at the center of the bond overlap (Figure 5d). Recalling that the stress pattern is that of the adherend's surface, the observed stress concentration may be due to "Poisson's ratio strains" in the adherends. That is, if the adherends are in uniform tension up to the bond area, there will be contraction of the thickness and width of the adherend in that bonded region.[9,12] This would be reflected in the adherend's stress pattern.

Finally, the fringe orders were approximately the same for all self-bonded samples ($2 \leq N \leq 3$). According to photoelastic theory, fringe orders, N, are related to material strain by:[5]

$$\varepsilon_x - \varepsilon_y = N(\lambda/2tK),$$

where ε_x and ε_y are the principal strains in the photoelastic coating and at the surface of the test part (nylon substrate), and t and K are, respectively, the thickness and strain-optical coefficient of the coating. Thus, there were similar levels of strain in all the self-bonded sample substrates. Stress, however, was not the same for each of the adherends in the different samples. Combining Hooke's Law, which relates stress and strain for elastic materials, with the above equation, gives the following:[2]

$$\sigma_x - \sigma_y = Nf\{E/(1+\nu)\}$$

where σ_x and σ_y are the principal stresses at the surface of the test part ($\sigma_y = 0$ if the stress state is uniaxial), ν is Poisson's ratio, $f = \lambda/2tK$, and E is the elastic modulus of the test part. Since the modulus of the GFN substrate was higher than that of the UFN substrate, the stress levels in the GFN substrate were greater than those in the UFN substrate. GFN samples sustained greater overall stress levels than UFN samples, and failed at higher applied loads, because peak stresses were lower, and the stress distribution more even, in the higher stiffness GFN coupon.

Cross-bonded samples. The photoelastic pattern for the more flexible substrate of the cross-bonded pair was identical to the pattern seen for the self-bonded samples. Pattern 2, for the stiffer substrate, initially developed in the same way as pattern 1. That is, color first appeared in the region of the coupon between the Instron grips and the top of the bonded area (Figure 6b). This was due to applied tensile load, and corresponding tensile strain in the coupon. Evidence of strain then moved into the bonded region (Figure 6c). High stress areas were again located at the top edges of the overlap (Figure 6c,d). The difference between patterns 1 and 2 was the location of the *second* high stress area. Rather than an area of stress concentration at the center of the bond overlap, a stress "front" appeared at the top of the overlap which spanned the width of the coupon, and which progressed down the length of the overlap with increasing load. If the stiffer coupon did not flex, during testing, to the extent that the more flexible coupon was able, the pattern for the stiffer coupon may be a result of greater, or continued, tensile straining of the coupon. Alternatively, the stiffness differential between the coupons may have caused different Poisson's ratio strains within the stiffer coupon. As for the self-bonded samples, with the exception of UFN/GFN samples (see below), fringe numbers for these cross-bonded samples were $2 \leq N \leq 3$. The failure initiation location (when observed) was at the bottom edges of the overlap.

As noted above, it was expected that GFN/MN samples would have higher strengths than UFN/GFN samples because of a greater disparity in substrate stiffness for the latter. This was not the case, however. Also, for the UFN/GFN samples, there was a significant difference in N for the two substrates. For the more flexible UFN substrate, N was of the order 2, while for the less flexible GFN substrate, N was of the order of 4. From this, and the difference in moduli, it appears that the GFN coupon was bearing more of the load than the UFN coupon. Therefore, it was the stiffness/modulus of the GFN material that determined the behavior of this sample, and the stiffness/modulus differential between the substrates was not a critical factor.

FINAL COMMENTS

The experiments detailed here have shown that substrate stiffness and modulus affect lap shear behavior by influencing the stress distribution patterns in the adhesive and adherends. It was demonstrated that photoelastic stress analysis, in conjuction with parametric analyses of theoretical models, is a useful technique for qualitively describing joint stress distribution for self- and cross-bonded samples. A single type of stress pattern was observed for the self-bonded samples regardless of substrate stiffness and modulus, while two types of patterns were seen for the cross-bonded samples. The predictions of the theoretical models and the results of the photoelastic analysis are in general agreement. Additionally, finite element analysis of these specific joints has been initiated.

Finally, it may be expected that in situations where actual automotive parts having complicated joint geometry or loading modes require analysis, and they are too complex to model effectively, a photoelastic investigation can provide valuable design and engineering information.

Acknowledgments

The author would like to thank K. S. Snavely and R. P. Schuler, Polymers Department, General Motors Research Laboratories, for help with sample preparation and testing. J. M. Frahm and B. E. Stevens, members of the General

Motors Corporation Advanced Engineering Staff, are also acknowledged for their help with the photoelastic equipment.

References

1. W. R. Risk, Society of Automotive Engineers, SP696, Paper No. 870281 (1987).
2. "Full-Field Interpretation," 030-Series Polariscope Instruction Manual, Photolastic Division, Measurements Group, Inc.
3. F. Zandman, S. Redner, and J. W. Dally, *Photoelastic Coatings* (Iowa State University Press and Society for Experimental Stress Analysis, Iowa, 1977).
4. J. W. Dally and W. F. Riley, *Experimental Stress Analysis* (McGraw-Hill New York, 1965), Part 3.
5. "Introduction to Stress Analysis by the Photostress Method," TN-702, Measurements Group, Inc. (1981).
6. W. J. Renton and J. R. Vinson, *J. Adhesion* **7**, 175 (1975).
7. L. J. Hart-Smith in *Developments in Adhesives-2,* A. J. Kinloch, Ed. (Applied Science Publishers, New Jersey, 1981).
8. J. A. Schroeder, unpublished results.
9. R. D. Adams and W. C. Wake, *Structural Adhesive Joints in Engineering* (Elsevier, New York, 1984), Chapter 2.
10. R. A. Kline in *Adhesive Joints*; *Formation, Characteristics, and Testing,* K. L. Mittal, Ed. (Plenum Press, New York, 1984).
11. H. Kyogoku, T. Sugibayashi, and K. Ikegami, *Trans. Jpn. Inst. Metals* **27** (2), 115 (1986).
12. R. D. Adams and N. A. Peppiatt, *J. Strain Analysis* **8**(2), 134 (1973).